Fast Complementary Filter for Attitude Estimation Using Low-Cost MARG Sensors

Article *in* IEEE Sensors Journal · September 2016

DOI: 10.1109/JSEN.2016.2589660

5 authors, including:

Jin Wu
The Hong Kong University of Science and Technology
95 PUBLICATIONS **526** CITATIONS
SEE PROFILE

Zebo Zhou
University of Electronic Science and Technology of China
54 PUBLICATIONS **669** CITATIONS
SEE PROFILE

Jingjun Chen
University of California, Davis
10 PUBLICATIONS **147** CITATIONS
SEE PROFILE

Hassen Fourati
University of Grenoble
88 PUBLICATIONS **1,028** CITATIONS
SEE PROFILE

Fast Complementary Filter for Attitude Estimation Using Low-Cost MARG Sensors

Jin Wu, *Student Member, IEEE*, Zebo Zhou, *Member, IEEE*, Jingjun Chen, Hassen Fourati, and Rui Li, *Member, IEEE*

***Abstract*— This paper proposes a novel quaternion-based attitude estimator with magnetic, angular rate, and gravity (MARG) sensor arrays. A new structure of a fixed-gain complementary filter is designed fusing related sensors. To avoid using iterative algorithms, the accelerometer-based attitude determination is transformed into a linear system. Stable solution to this system is obtained via control theory. With only one matrix multiplication, the solution can be computed. Using the increment of the solution, we design a complementary filter that fuses gyroscope and accelerometer together. The proposed filter is fast, since it is free of iteration. We name the proposed filter the fast complementary filter (FCF). To decrease significant effects of unknown magnetic distortion imposing on the magnetometer, a stepwise filtering architecture is designed. The magnetic output is fused with the estimated gravity from gyroscope and accelerometer using a second complementary filter when there is no significant magnetic distortion. Several experiments are carried out on real hardware to show the performance and some comparisons. Results show that the proposed FCF can reach the accuracy of Kalman filter. It successfully finds a balance between estimation accuracy and time consumption. Compared with iterative methods, the proposed FCF has much less convergence speed. Besides, it is shown that the magnetic distortion would not affect the estimated Euler angles.**

***Index Terms*— MARG sensors, attitude estimation, fast complementary filter, magnetic distortion, Kalman filter.**

I. Introduction

INTELLIGENT measurement techniques have been extensively adopted in many areas [1]. MARG sensors, often consist of 3-axis MEMS gyroscope, accelerometer and magnetometer, are widely used in many applications of attitude determination e.g. human motion tracking, Unmanned Aerial Vehicle (UAV), mobile navigation and etc. [2]–[4]. MEMS gyroscope measures the angular rate of a moving object in terms of inertial principles. MEMS accelerometer provides the acceleration of a certain object using Newton's laws. Magnetometer produces the sensing of the geomagnetic field. Different from the conventional inertial sensors e.g. Fibre-Optic Gyroscope (FOG), Ring-Laser Gyroscope (RLG) and etc., MEMS inertial sensors' performances always suffer from their inherent drawbacks [5], [6], e.g. nonlinearity, random walk, temperature drift and etc., which means we can not just rely on a single MEMS inertial sensor to obtain accurate attitude estimation [7]. To ensure a reliable attitude solution, MARG sensors have to be fused together using optimal sensor fusion algorithms [8], [9].

In the past decades, sensor fusion has been well developed so far that consequently generates many useful products. For instance, Li et al. proposed an efficient variance component estimation method which observably improves the computation speed of the multi-sensor fusion [10]. For industrial production, price is a crucial standard for choosing source components of an attitude measuring platform. Therefore for low-cost MARG sensors, they tremendously boost the development of many related applications like mobile phones, smart wearables and wireless sensing. Looking back on existing methods, we can categorize them into two sorts: One mainly includes complementary filters [11]–[17] and the other relates to Kalman filtering [3], [18]–[21]. Complementary filter (CF) is relatively simple and easy to be applied while Kalman filter (KF) needs more complex matrix operations and can hardly be implemented on platforms with low hardware configurations [22]. Hence, in this paper, we focus on CF for attitude estimation.

When the motion of a certain object remains smooth, the accelerometer's output approximates the gravity of the object, i.e the attitude calculated from accelerometer and magnetometer is relatively accurate and reliable at this time. Meanwhile, due to the drift of the MEMS gyroscope, the attitude from gyro integration diverges within a very short period. When the motion ceases to be flat, accelerometer's output will be disturbed by non-gravitational acceleration which makes the calculated attitude unreliable. At this time, the gyroscope will compensate for such errors. Such frequency behaviour of the two inertial sensors indicates that accelerometer and gyroscope can compensate for each other in the frequency domain. This is

Manuscript received April 15, 2016; revised July 2, 2016; accepted July 6, 2016. Date of publication July 9, 2016; date of current version August 15, 2016. This work was supported in part by the Key Laboratory of Precise Engineering and Industry Surveying of the National Administration of Surveying, Mapping and Geoinformation under Grant PF2015-11, in part by the NASG Key Laboratory of Land Environment and Disaster Monitoring under Grant LEDM2014B09, and in part by the National Natural Science Foundation of China under Grant 61450010. The associate editor coordinating the review of this paper and approving it for publication was Dr. Akshya Swain. *(Corresponding author: Zebo Zhou.)*

J. Wu is with the School of Aeronautics and Astronautics and School of Automation, University of Electronic Science and Technology of China, Chengdu 611731, China (e-mail: jin_wu_uestc@hotmail.com).

Z. Zhou is with the School of Aeronautics and Astronautics, University of Electronic Science and Technology of China, Chengdu 611731, China (e-mail: klinsmann.zhou@gmail.com).

J. Chen is with the Department of Electrical and Computer Engineering, University of California at Davis, Davis, CA 95616 USA (e-mail: chenjingjun.ee@hotmail.com).

H. Fourati is with the Grenoble-Image-Speech-Signal-Automatics Laboratory, Centre National de la Recherche Scientifique, University Grenoble Alpes, Grenoble 38400, France, and also with Inria, Le Chesnay 78153, France (e-mail: hassen.fourati@gipsa-lab.grenoble-inp.fr).

R. Li is with the School of Automation, University of Electronic Science and Technology of China, Chengdu 611731, China (e-mail: hitlirui@gmail.com).

Digital Object Identifier 10.1109/JSEN.2016.2589660

the fundamental principle of attitude estimation from MARG sensors using CF.

In fact, such filtering has been studied for quite a long time e.g. some early thoughts were by Gebre-Egziabher [23]. During the recent ten years, many related methods have been developed. Most of them use the strategy that the accelerometer and magnetometer are used in the way of measurement fusion. It should be noted that the combination of 3-axis accelerometer and magnetometer is widely referred to as the electronic compass [24], [25]. Corresponding fusion equation and vector observations in the North-East-Down (NED) frame are given by

$$\begin{cases} \mathbf{A}^b = \mathbf{C}\mathbf{A}^r \\ \mathbf{M}^b = \mathbf{C}\mathbf{M}^r, \end{cases} \quad \begin{cases} \mathbf{A}^b = (a_x, a_y, a_z)^T \\ \mathbf{A}^r = (0, 0, 1)^T \\ \mathbf{M}^b = (m_x, m_y, m_z)^T \\ \mathbf{M}^r = (m_N, 0, m_D)^T \end{cases} \tag{1}$$

where $\mathbf{A}^b, \mathbf{M}^b$ and $\mathbf{A}^r, \mathbf{M}^r$ denote the observation vectors of accelerometer and magnetometer in the body frame b and reference frame r respectively. $\mathbf{C}$ stands for the Direction Cosine Matrix (DCM). Equations in (1) can also be represented with quaternion as follows

$$\begin{cases} 2(q_1q_3 - q_0q_2) - a_x = 0 \\ 2(q_0q_1 + q_2q_3) - a_y = 0 \\ (q_0^2 - q_1^2 - q_2^2 + q_3^2) - a_z = 0 \\ m_N(q_0^2 + q_1^2 - q_2^2 - q_3^2) + 2m_D(q_1q_3 - q_0q_2) - m_x = 0 \\ 2m_N(q_1q_2 - q_0q_3) + 2m_D(q_0q_1 + q_2q_3) - m_y = 0 \\ 2m_N(q_0q_2 + q_1q_3) + m_D(q_0^2 - q_1^2 - q_2^2 + q_3^2) - m_z = 0 \end{cases} \tag{2}$$

and can be solved by means of iterative methods like Gradient Descent Algorithm (GDA) [14], Gauss Newton Algorithm (GNA) [16], [26], Levenberg-Marquadt Algorithm (LMA) [13], [27] and etc. Besides, the accelerometer-magnetometer fusion can be solved with solutions to the Wahba's problem [28]. For instance, Markley derived the closed-form solution to the Wahba's problem from two vector observations [29]. Using geometric relationships, this problem can be solved using TRIAD [30], Yun's FQA [12], [31] as well.

The above algorithms are mostly efficient. However, there are still drawbacks. Iterative methods consume too much in terms of time and space costs. Also,attitude estimation performances in the presence of large external acceleration and magnetic distortion are not always satisfactory. Motivated by the methods listed above, we propose a novel CF that owns low time consumption. The main contributions of this paper are listed as follows:

1) The accelerometer-based attitude determination problem is transformed into a linear system. The obtained stable solution to the system is subsquently used as measurement in the CF.
2) A new structure of the CF is designed, as shown in Fig. 1. The accelerometer and gyroscope are fused first to estimate gravity.
3) Magnetic distortion detection is introduced. The magnetometer's output is fused with estimated gravity based on Markley's algorithm [32] and a second CF. The block diagram is shown in Fig. 3.
4) Experiments are carried out to show the efficiency of the proposed fast CF (FCF) regarding attitude estimation accuracy, anti-vibration ability, time consumption and convergence speed, compared with representative methods and golden reference.

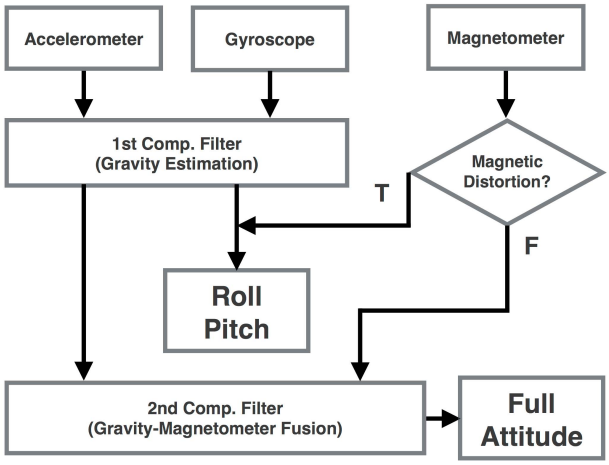

Fig. 1. Basic structure of the proposed FCF.

In this way, the proposed method aims to give a better and more robust estimation of gravity and heading.

This paper has the following arrangement of contents: Section II gives the brief knowledge of CF. Section III contains the details of the proposed gravity estimation theory. Section IV involves the gravity-magnetometer fusion scheme. Section V presents the experiments and comparison results. Concluding remarks are given in Section VI.

II. Brief of Complementary Filter

To unite the usage of mathematical symbols, this paper uses basically the same mathematical expressions like quaternion, angular rate, field discription and etc. as that adopted by [14] and [16].

A 3-axial gyroscope measures the 3D angular rate of a certain object in its body frame such that it can be defined by

$$\omega = (\omega_x, \omega_y, \omega_z)^T \tag{3}$$

For a rigid body, its rotation can be represented by quaternion. A very frequently used relationship between quaternion and the angular rate can be expressed by the following ordinary differential equation

$$\begin{aligned} \frac{d\mathbf{q}_{\omega,t}}{dt} &= \frac{1}{2}\left[\Omega\times\right]\mathbf{q}_{\omega,t-1} \\ &= \frac{1}{2}\begin{pmatrix} 0 & -\omega_x & -\omega_y & -\omega_z \\ \omega_x & 0 & \omega_z & -\omega_y \\ \omega_y & -\omega_z & 0 & \omega_x \\ \omega_z & \omega_y & -\omega_x & 0 \end{pmatrix}\mathbf{q}_{\omega,t-1} \end{aligned} \tag{4}$$

where $\mathbf{q}_{\omega,t}$ is the quaternion calculated through gyroscope integration at the time epoch t. MEMS gyroscope has considerable random walk that consequently produces a drift of integration within a short period. Hence, a 3-axial

accelerometer is introduced to compensate for the error of the angular rate. As implemented by Madgwick *et al.* [14] and Tian *et al.* [16], the first order CF model is given by

$$\mathbf{q}_{est,t} = (1-\gamma)\mathbf{q}_{\omega,t} + \gamma\,\mathbf{q}_{measure,t},\ \gamma \in (0,1) \tag{5}$$

where γ is the gain for the CF. $\mathbf{q}_{est,t}$ stands for the estimated quaternion at time epoch t.

III. Gravity Estimation

A. Quaternion From Accelerometer

Now we consider the accelerometer compensation strategy. The rotation equation with the accelerometer can be extracted from (1) as

$$\mathbf{A}^b = \mathbf{C}\mathbf{A}^r \tag{6}$$

Remark 1: A direction cosine matrix (DCM) can be written in the following form

$$\mathbf{C} = (\mathbf{C}_1, \mathbf{C}_2, \mathbf{C}_3) \tag{7}$$

where $\mathbf{C}_i$ $(i = 1, 2, 3)$ denotes the ith column of the DCM. Each column can be represented with

$$\begin{aligned}\mathbf{C}_1 &= \begin{pmatrix} q_0^2+q_1^2-q_2^2-q_3^3 \\ 2q_1q_2-2q_0q_3 \\ 2q_0q_2+2q_1q_3 \end{pmatrix} \\ &= \begin{pmatrix} q_0 & q_1 & -q_2 & -q_3 \\ -q_3 & q_2 & q_1 & -q_0 \\ q_2 & q_3 & q_0 & q_1 \end{pmatrix}\begin{pmatrix} q_0 \\ q_1 \\ q_2 \\ q_3 \end{pmatrix} = \mathbf{P}_1\mathbf{q} \end{aligned} \tag{8}$$

$$\begin{aligned}\mathbf{C}_2 &= \begin{pmatrix} 2q_1q_2+2q_0q_3 \\ q_0^2-q_1^2+q_2^2-q_3^2 \\ -2q_0q_1+2q_2q_3 \end{pmatrix} \\ &= \begin{pmatrix} q_3 & q_2 & q_1 & q_0 \\ q_0 & -q_1 & q_2 & -q_3 \\ -q_1 & -q_0 & q_3 & q_2 \end{pmatrix}\begin{pmatrix} q_0 \\ q_1 \\ q_2 \\ q_3 \end{pmatrix} = \mathbf{P}_2\mathbf{q} \end{aligned} \tag{9}$$

$$\begin{aligned}\mathbf{C}_3 &= \begin{pmatrix} -2q_0q_2+2q_1q_3 \\ 2q_2q_3+2q_0q_1 \\ q_0^2-q_1^2-q_2^2+q_3^2 \end{pmatrix} \\ &= \begin{pmatrix} -q_2 & q_3 & -q_0 & q_1 \\ q_1 & q_0 & q_3 & q_2 \\ q_0 & -q_1 & -q_2 & q_3 \end{pmatrix}\begin{pmatrix} q_0 \\ q_1 \\ q_2 \\ q_3 \end{pmatrix} = \mathbf{P}_3\mathbf{q} \end{aligned} \tag{10}$$

Hence (6) can be decomposed such as

$$\begin{aligned}\mathbf{A}^b &= \mathbf{C}\mathbf{A}^r \\ &\Leftrightarrow (\mathbf{C}_1, \mathbf{C}_2, \mathbf{C}_3)\begin{pmatrix} 0 \\ 0 \\ 1 \end{pmatrix} = \mathbf{A}^b \\ &\Leftrightarrow \mathbf{P}_3\mathbf{q}_a = \mathbf{A}^b \end{aligned} \tag{11}$$

where $\mathbf{q}_a$ denotes the quaternion from accelerometer. The equation is then transformed into

$$\mathbf{q}_a = \mathbf{P}_3^{\dagger}\mathbf{A}^b \tag{12}$$

where † stands for the Moore-Penrose pseudo-inverse matrix [33].

Theorem 1: $\mathbf{P}_1^T = \mathbf{P}_1^{\dagger}, \mathbf{P}_2^T = \mathbf{P}_2^{\dagger}, \mathbf{P}_3^T = \mathbf{P}_3^{\dagger}$

Proof:

$$\begin{aligned}\mathbf{P}_1\mathbf{P}_1^T &= \mathbf{P}_2\mathbf{P}_2^T = \mathbf{P}_3\mathbf{P}_3^T \\ &= (q_0^2+q_1^2+q_2^2+q_3^2)\mathbf{I}_{3\times3} = \mathbf{I}_{3\times3} \\ \Leftrightarrow \mathbf{P}_1^T &= \mathbf{P}_1^{\dagger}, \mathbf{P}_2^T = \mathbf{P}_2^{\dagger}, \mathbf{P}_3^T = \mathbf{P}_3^{\dagger} \end{aligned} \tag{13}$$

This generates Theorem 1. ■

With Theorem 1, (12) becomes

$$\begin{aligned}\mathbf{q}_a &= \mathbf{P}_3^{\dagger}\mathbf{A}^b = \mathbf{P}_3^T\mathbf{A}^b \\ &\Rightarrow \begin{pmatrix} q_0 \\ q_1 \\ q_2 \\ q_3 \end{pmatrix} = \begin{pmatrix} -a_xq_2+a_yq_1+a_zq_0 \\ a_xq_3+a_yq_0-a_zq_1 \\ -a_xq_0+a_yq_3-a_zq_2 \\ a_xq_1+a_yq_2+a_zq_3 \end{pmatrix} \\ &\Rightarrow \begin{pmatrix} a_z-1 & a_y & -a_x & 0 \\ a_y & -a_z-1 & 0 & a_x \\ -a_x & 0 & -a_z-1 & a_y \\ 0 & a_x & a_y & a_z-1 \end{pmatrix}\mathbf{q}_a = \mathbf{0} \end{aligned} \tag{14}$$

Define $\mathbf{W}_a$ as

$$\mathbf{W}_a = \begin{pmatrix} a_z & a_y & -a_x & 0 \\ a_y & -a_z & 0 & a_x \\ -a_x & 0 & -a_z & a_y \\ 0 & a_x & a_y & a_z \end{pmatrix} \tag{15}$$

(14) becomes

$$\mathbf{W}_a\mathbf{q}_a = \mathbf{q}_a \tag{16}$$

Theorem 2: $\mathbf{q}_a = \frac{\mathbf{W}_a+\mathbf{I}_{4\times4}}{2}\mathbf{q}_0$ *satisfies (16) for any randomly chosen* $\mathbf{q}_0$.

Proof: (16) can be seen as an iterative equation for $\mathbf{q}$, such that

$$\mathbf{q}_a(t) = \mathbf{W}_a\mathbf{q}_a(t-1) \tag{17}$$

However, note that

$$\mathbf{W}_a^2 = \begin{pmatrix} \|\mathbf{A}^b\|^2 & 0 & 0 & 0 \\ 0 & \|\mathbf{A}^b\|^2 & 0 & 0 \\ 0 & 0 & \|\mathbf{A}^b\|^2 & 0 \\ 0 & 0 & 0 & \|\mathbf{A}^b\|^2 \end{pmatrix} = \mathbf{I}_{4\times4} \tag{18}$$

Apparently, (17) is not feasible to calculate the quaternion. As the matter of fact, (17) can be seen as a linear discrete constant dynamical system. If so, it can be transformed into a continuous system. According to modern control theory, a linear discrete constant system can be transform into

$$\mathbf{q}_a(t) = \mathbf{W}_a\mathbf{q}_a(t-1) \Rightarrow \frac{d\mathbf{q}_a}{dt} = \mathbf{H}_a\mathbf{q}_a \tag{19}$$

if and only if

$$\mathbf{W}_a = e^{\mathbf{H}_aT} \tag{20}$$

where T denotes the sampling interval. As there are zero items in $\mathbf{W}_a$, the natural logarithm of $\mathbf{W}_a$ may contains $-\infty$ items, which makes no sense for $\mathbf{H}_a$. Hence, to approximately get $\mathbf{H}_a$, we use the first-order Taylor expansion of $e^{\mathbf{H}_aT}$, such that

$$\mathbf{W}_a = \mathbf{I}_{4\times4} + \mathbf{H}_aT \tag{21}$$

which generates the approximated $\mathbf{H}_a$

$$\mathbf{H}_a \approx \frac{\mathbf{W}_a - \mathbf{I}_{4\times4}}{T} \tag{22}$$

where the time interval T is chosen very small. Thus the continuous form of (17) becomes

$$\frac{d\mathbf{q}_a}{dt} = \frac{\mathbf{W}_a - \mathbf{I}_{4\times4}}{T}\mathbf{q}_a \tag{23}$$

The solution to this continuous system can be derived as

$$\mathbf{q}_a = e^{\mathbf{H}_a t}\mathbf{q}_0 \tag{24}$$

where, the exponential part is calculated by

$$e^{\mathbf{H}_a t} = \mathbf{I}_{4\times4} + \mathbf{H}_a t + \frac{\mathbf{H}_a^2 t^2}{2!} + \cdots \frac{\mathbf{H}_a^n t^n}{n!} \tag{25}$$

where

$$\begin{aligned}
\mathbf{H}_a^2 &= (\frac{\mathbf{W}_a - \mathbf{I}_{4\times4}}{T})(\frac{\mathbf{W}_a - \mathbf{I}_{4\times4}}{T}) \\
&= \frac{\mathbf{W}_a^2 - 2\mathbf{W}_a + \mathbf{I}_{4\times4}}{T^2} = -2\frac{\mathbf{W}_a - \mathbf{I}_{4\times4}}{T^2} = -\frac{2}{T}\mathbf{H}_a \\
\Rightarrow \mathbf{H}_a^3 &= \frac{4}{T^2}\mathbf{H}_a \\
\Rightarrow \mathbf{H}_a^n &= \left(\frac{-2}{T}\right)^{n-1}\mathbf{H}_a
\end{aligned} \tag{26}$$

In this way $e^{\mathbf{H}_a t}$ can be rewritten such as

$$\begin{aligned}
e^{\mathbf{H}_a t} &= \mathbf{I}_{4\times4} + \mathbf{H}_a t + \frac{\mathbf{H}_a^2 t^2}{2!} + \cdots \frac{\mathbf{H}_a^n t^n}{n!} \\
&= \mathbf{I} + \mathbf{H}_a t - \frac{\frac{2}{T}}{2!}\mathbf{H}_a t^2 + \frac{\frac{4}{T^2}}{3!}\mathbf{H}_a t^3 + \cdots \\
&= \mathbf{I} + \mathbf{H}_a\left(t - \frac{\frac{2}{T}}{2!}t^2 + \frac{\frac{4}{T^2}}{3!}t^3 + \cdots\right)
\end{aligned} \tag{27}$$

Let

$$p = \left(t - \frac{\frac{2}{T}}{2!}t^2 + \frac{\frac{4}{T^2}}{3!}t^3 + \cdots\right) \tag{28}$$

we have

$$\begin{aligned}
-\frac{2}{T}p &= -\frac{2}{T}t + \frac{\left(-\frac{2}{T}t\right)^2}{2!} + \frac{\left(-\frac{2}{T}t\right)^3}{3!} + \cdots \\
&= e^{-\frac{2}{T}t} - 1 \\
\Rightarrow p &= \frac{T}{2} - \frac{T}{2}e^{-\frac{2}{T}t}
\end{aligned} \tag{29}$$

Hence

$$e^{\mathbf{H}_a t} = \mathbf{I}_{4\times4} + \left(\frac{T}{2} - \frac{T}{2}e^{-\frac{2}{T}t}\right)\mathbf{H}_a \tag{30}$$

when $t \to +\infty$, it turns to be

$$\lim_{t\to+\infty} e^{\mathbf{H}_a t} = \mathbf{I}_{4\times4} + \frac{T}{2}\mathbf{H}_a \tag{31}$$

Given any $\mathbf{q}_0$, the solution can be given by

$$\mathbf{q}_a = e^{\mathbf{H}_a t}\mathbf{q}_0 = \left(\mathbf{I}_{4\times4} + \frac{T}{2}\mathbf{H}_a\right)\mathbf{q}_0 = \frac{\mathbf{W}_a + \mathbf{I}_{4\times4}}{2}\mathbf{q}_0 \tag{32}$$

■

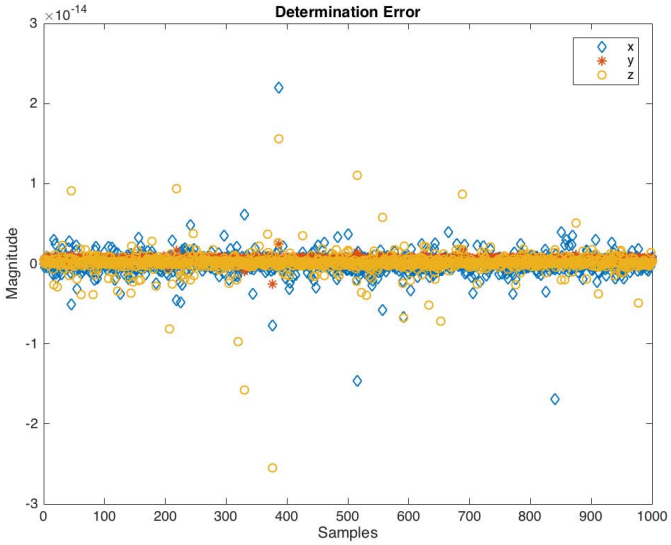

Fig. 2. Computation error **e**. The x axis denotes the sampling number index while the y axis represents the error scalar.

Remark 2: Particularly, if $\mathbf{q}_0 = (1, 0, 0, 0)^T$, it arrives at

$$\mathbf{q}_a = \frac{\mathbf{W}_a + \mathbf{I}}{2}\mathbf{q}_0 = \frac{1}{2}\begin{pmatrix} a_z + 1 & a_y & -a_x & 0 \end{pmatrix}^T \tag{33}$$

After normalization, we obtain

$$\mathbf{q}_a = \pm\frac{1}{\sqrt{(a_z+1)^2 + a_y^2 + a_x^2}}(a_z + 1, a_y, -a_x, 0)^T \tag{34}$$

Remark 3: This finding gives us an important piece of information that the quaternion from accelerometer can be computed with (32) immediately. Here, we would like to conduct a numerical simulation to illustrate this equation. Then, the numerical simulation generates unit quaternions randomly and they are served as different initial values for (32). Accelerometer outputs are randomly set as $a_x = -0.01590$, $a_y = 0.99408$, $a_z = -0.10751$. Using the calculated quaternions, the correponding normalized acceleration can be calculated with

$$\begin{cases} 2(q_1q_3 - q_0q_2) = \hat{a}_x \\ 2(q_0q_1 + q_2q_3) = \hat{a}_y \\ (q_0^2 - q_1^2 - q_2^2 + q_3^2) = \hat{a}_z \end{cases} \tag{35}$$

The computation error is given by

$$\mathbf{e} = \begin{pmatrix} \hat{a}_x - a_x, \hat{a}_y - a_y, \hat{a}_z - a_z \end{pmatrix}^T \tag{36}$$

The simulation results are shown in Fig 2. As can be seen from the above figure, the scale of the computation error is about 1×10^{-14} which is tiny enough to be ignored.

Remark 4: The quaternion increment is given by

$$\mathbf{q}_a = \tfrac{\mathbf{W}_a+\mathbf{I}}{2}\mathbf{q}_0 \Rightarrow \Delta\mathbf{q}_a = \tfrac{\mathbf{W}_a-\mathbf{I}}{2}\mathbf{q}_0 \tag{37}$$

B. Gravity Filter

The estimation of quaternion in (5) can also be described as (38)

$$\mathbf{q}_{est,a\omega,t} = \hat{\mathbf{q}}_{est,a\omega,t-1} + \dot{\mathbf{q}}_{a\omega,t}\Delta t \tag{38}$$

where $\dot{\mathbf{q}}_{a\omega,t}$ denotes the fused direction rate by accelerometer and gyroscope which is defined by (39):

$$\dot{\mathbf{q}}_{a\omega,t} = (1-\gamma)\dot{\mathbf{q}}_{\omega,t} + \gamma\,\dot{\mathbf{q}}_{a,t},\ \gamma \in (0,1) \tag{39}$$

where, γ denotes the complementary gain. (38) can be further expressed as

$$\begin{aligned}
&\mathbf{q}_{est,a\omega,t} \\
&= \hat{\mathbf{q}}_{est,a\omega,t-1} + \dot{\mathbf{q}}_{a\omega,t}\,\Delta t \\
&= \hat{\mathbf{q}}_{est,a\omega,t-1} + \left[(1-\gamma)\dot{\mathbf{q}}_{\omega,t} + \gamma\,\dot{\mathbf{q}}_{a,t}\right]\Delta t \\
&= \hat{\mathbf{q}}_{est,t-1} + \frac{(1-\gamma)}{2}\,[\Omega\times]\,\hat{\mathbf{q}}_{est,a\omega,t-1}\Delta t + \gamma\,\Delta\mathbf{q}_{a,t} \\
&= \left\{\frac{(1-\gamma)\Delta t}{2}\,[\Omega\times] + \mathbf{I}\right\}\hat{\mathbf{q}}_{est,a\omega,t-1} + \gamma\,\frac{\mathbf{W}_a - \mathbf{I}}{2}\hat{\mathbf{q}}_{est,a\omega,t-1} \\
&= \left\{\mathbf{I} + \frac{(1-\gamma)\Delta t}{2}\,[\Omega\times] + \gamma\,\frac{\mathbf{W}_a - \mathbf{I}}{2}\right\}\hat{\mathbf{q}}_{est,a\omega,t-1}
\end{aligned} \tag{40}$$

which is the final accelerometer-gyroscope update equation for the proposed CF. Notice that a normalization step should be performed after each update

$$\hat{\mathbf{q}}_{est,a\omega,t} = \frac{\mathbf{q}_{est,a\omega,t}}{\left\|\mathbf{q}_{est,a\omega,t}\right\|} \tag{41}$$

During each update period, the quaternion $\mathbf{q}_{est,a\omega,t}$ and estimated gravity $\mathbf{G}_t^b$ can be obtained. The estimated gravity can be given by

$$\mathbf{G}_t^b = \mathbf{C}(\hat{\mathbf{q}}_{est,a\omega,t})\mathbf{A}^r \tag{42}$$

IV. Gravity and Magnetometer Fusion

Attitude determination from two vector observations can be achieved via analytic method proposed by Markley [29]. The closed form of the optimal quaternion $\mathbf{q}_{opt}$ can be expressed as:

$$\mathbf{q} = \frac{1}{2\sqrt{\varsigma(\varsigma+|\rho|)(1+\mathbf{b}_\times\cdot\mathbf{r}_\times)}} \begin{cases} \begin{bmatrix} (\varsigma+\rho)(\mathbf{b}_\times\times\mathbf{r}_\times) + \sigma(\mathbf{b}_\times+\mathbf{r}_\times) \\ (\varsigma+\rho)(1+\mathbf{b}_\times\cdot\mathbf{r}_\times) \end{bmatrix}, \rho \geq 0 \\ \begin{bmatrix} \sigma(\mathbf{b}_\times\times\mathbf{r}_\times) + (\varsigma-\rho)(\mathbf{b}_\times+\mathbf{r}_\times) \\ \sigma(1+\mathbf{b}_\times\cdot\mathbf{r}_\times) \end{bmatrix}, \rho < 0 \end{cases} \tag{43}$$

with the parameters of

$$\begin{aligned}
\rho &= (1+\mathbf{b}_\times\cdot\mathbf{r}_\times)[\tilde{w}\mathbf{b}_1\cdot\mathbf{r}_1 + (1-\tilde{w})\mathbf{b}_2\cdot\mathbf{r}_2] \\
&\quad + [\mathbf{b}_\times\times\mathbf{r}_\times)\cdot(\tilde{w}\mathbf{b}_1\times\mathbf{r}_1 + (1-\tilde{w})\mathbf{b}_2\times\mathbf{r}_2] \\
\sigma &= (\mathbf{b}_\times+\mathbf{r}_\times)\cdot[\tilde{w}\mathbf{b}_1\times\mathbf{r}_1 + (1-\tilde{w})\mathbf{b}_2\times\mathbf{r}_2] \\
\varsigma &= \sqrt{\rho^2+\sigma^2}
\end{aligned} \tag{44}$$

where $\tilde{w}$ denotes the weight of the first vector observation.

In this case, the vectors $\mathbf{b}_1$, $\mathbf{r}_1$, $\mathbf{b}_2$, $\mathbf{r}_2$, $\mathbf{r}_\times$ and $\mathbf{b}_\times$ are defined as:

$$\begin{cases} \mathbf{b}_1 = \mathbf{G}^b = (g_x, g_y, g_z)^T \\ \mathbf{r}_1 = \mathbf{A}^r = (0,0,1)^T \\ \mathbf{b}_2 = \mathbf{M}^b = (m_x, m_y, m_z)^T \\ \mathbf{r}_2 = \mathbf{M}^r = (m_N, 0, m_D)^T \\ \mathbf{r}_\times = \dfrac{\mathbf{r}_1\times r_2}{\|\mathbf{r}_1\times\mathbf{r}_2\|} \\ \mathbf{b}_\times = \dfrac{\mathbf{b}_1\times\mathbf{b}_2}{\|\mathbf{b}_1\times\mathbf{b}_2\|} \end{cases} \tag{45}$$

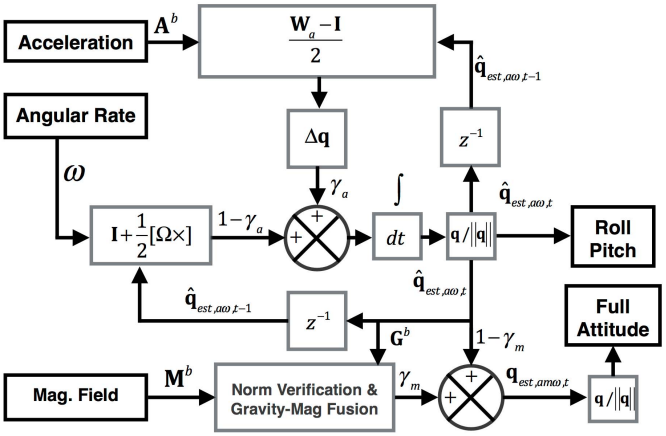

Fig. 3. Complementary filter structure for accelerometer and gyroscope fusion, where the accelerometer is used as measurement source which compensates for the error induced by gyroscope's random drift.

where $\mathbf{G}^b$ represents the compensated gravity vector from the CF proposed in last section. This fusion method requires a highly accurate measurement of magnetic direction in the reference frame $\mathbf{M}^r$. Common solution is to compensate for the reference vector with know magnetic map. However this may not be easily acquired in some special environments. Since an piece of information is extracted from the sensor fusion

$$\begin{aligned}
\left(\mathbf{G}^b\right)^T\mathbf{M}^b &= \left(\mathbf{C}\mathbf{A}^r\right)^T\mathbf{C}\mathbf{M}^r \\
&= \left(\mathbf{A}^r\right)^T\mathbf{C}^T\mathbf{C}\mathbf{M}^r \\
&= \left(\mathbf{A}^r\right)^T\mathbf{M}^r \\
&\Rightarrow m_D = g_x m_x + g_y m_y + g_z m_z \\
&\Rightarrow m_N = \sqrt{1-m_D^2}
\end{aligned} \tag{46}$$

this problem can be solved without reference vectors. Using the above introduced method, the quaternion from the gravity and magnetic sensing can be obtained. However, due to the noise spectrum of the magnetometer, the determined quaternion is not smooth enough. In this way, a filter should be adopted to smooth the estimates. Let the gravity-magnetic quaternion be $\mathbf{q}_{gm}$ and the estimated full-attitude estimator produces $\mathbf{q}_{am\omega}$. Then the magnetometer-based quaternion is filtered via

$$\mathbf{q}_{est,am\omega,t} = (1-\gamma_m)\hat{\mathbf{q}}_{est,a\omega,t} + \gamma_m\mathbf{q}_{gm,t} \tag{47}$$

where γ_m denotes the filter gain. Step normalization generates the full-attitude estimation

$$\hat{\mathbf{q}}_{est,am\omega,t} = \frac{\mathbf{q}_{est,am\omega,t}}{\left\|\mathbf{q}_{est,am\omega,t}\right\|} \tag{48}$$

Note that the gravity-magnetometer fusion is only conducted when the magnetic field is stable. The external magnetic distortion can be detected via the norm of the magnetic field. The overall block diagram of the proposed CF is shown in Fig. 3. The pseudocode of the FCF is given as follows in Algorithm 1.

Algorithm 1: Proposed Fast Complementary Filter (FCF) With Acceleration, Angular Rate and Magnetic Field Inputs

Initialize: $t = 0, \hat{\mathbf{q}}_{est,a\omega,t=0} = \hat{\mathbf{q}}_{est,am\omega,t=0} = (1,0,0,0)^T$.
while no stop commands received **and** at least gyroscope valid **do**

1) **Input:** $\omega, \mathbf{A}^b, \mathbf{M}^b$
2) $t = t + 1, \mathbf{A}^b = \frac{\mathbf{A}^b}{\|\mathbf{A}^b\|}$
3) $\mathbf{q}_{est,a\omega,t} = \left\{\mathbf{I} + \frac{(1-\gamma_a)\Delta t}{2}[\Omega\times] + \gamma_a \frac{\mathbf{W}_a - \mathbf{I}}{2}\right\} \hat{\mathbf{q}}_{est,a\omega,t-1}$
4) $\hat{\mathbf{q}}_{est,a\omega,t} = \frac{\mathbf{q}_{est,a\omega,t}}{\|\mathbf{q}_{est,a\omega,t}\|}$
5) **If** $\|\mathbf{M}^b\|$ too big or too small
   Output: $\hat{\mathbf{q}}_{est,a\omega,t}$
   Continue to next loop.
   Else, $\mathbf{G}^b = \mathbf{C}(\hat{\mathbf{q}}_{est,a\omega,t})\mathbf{A}^r, \mathbf{M}^b = \frac{\mathbf{M}^b}{\|\mathbf{M}^b\|}$.
6) Perform gravity-magnetometer fusion with (43) and calculate $\mathbf{q}_{gm,t}$.
7) $\mathbf{q}_{est,am\omega,t} = (1-\gamma_m)\hat{\mathbf{q}}_{est,a\omega,t} + \gamma_m \mathbf{q}_{gm,t}$
8) $\hat{\mathbf{q}}_{est,am\omega,t} = \frac{\mathbf{q}_{est,am\omega,t}}{\|\mathbf{q}_{est,am\omega,t}\|}$
9) **Output:** $\hat{\mathbf{q}}_{est,am\omega,t}$

end while

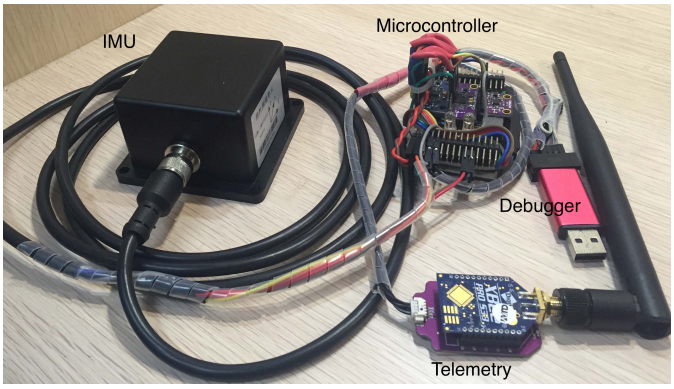

Fig. 4. ADIS16405 IMU, STM32F405 microcontroller, a Xbee Pro S3B 900Mhz telemetry and a USB SWD debugger.

V. Experiments and Results

A. Platform Description for Experiments

A MEMS based Inertial Measurement Unit (IMU) platform is designed to conduct various experiments (see Fig. 4). The platform consists of a high precision IMU ADIS16405 produced by Analog Device Inc [34]. The output of gyroscope, accelerometer and magnetometer can be acquired. An embedded microcontroller STM32F405 is attached to this IMU via Serial Peripheral Interface (SPI) to conduct robust data acquisition with high sampling frequency. All comparisons are obtained on a Macbook Pro laptop with a CPU of 4-core i7-4770HQ. The MATLAB r2015 software is used for data processing and analysis. Furthermore, an accurate MTi Xsens Attitude and Heading Reference System (AHRS) is connected to the microcontroller to generate golden reference Euler angles.

B. Common Attitude Estimation Test

The samples are collected by using the designed equipment and the raw data is drawn in Fig. 5. In this case, there is no magnetic distortion and the motion is relatively smooth. Using the FCF proposed in the previous section, the 3D attitude of the IMU is calculated. Yet, to compare with the KF-based methods, a recently developed Linear Kalman Filter (LKF) proposed by Valenti *et al.* [21] is employed here. Valenti's method has the least numbers of state variables which makes it faster than other KF-based attitude estimator with more state variables. The three Euler angles from different sources are plotted in Fig. 6.

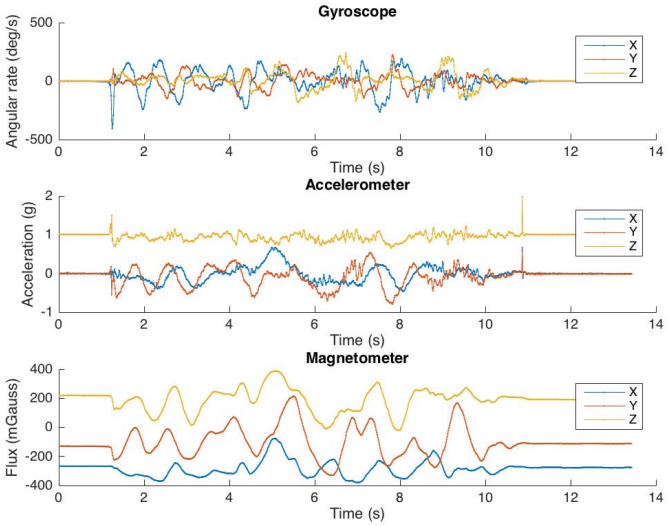

Fig. 5. Raw data which includes gyroscope, accelerometer and magnetometer's outputs.

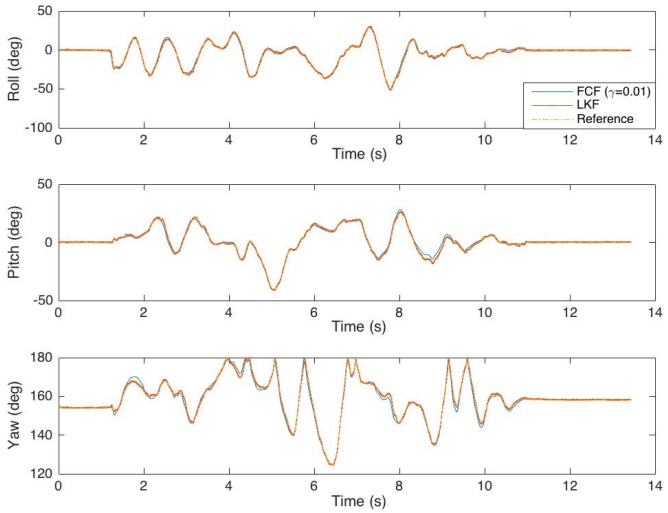

Fig. 6. Euler angles from the proposed FCF ($\gamma_a = \gamma_m = 0.01$), Valenti's LKF method and MTi-Xsens's reference.

The errors of the respective Euler angles are computed as the difference from that of the golden reference. The comparison on Euler angles errors of FCF and KF are ploted in Fig. 7. These plots show that the proposed FCF with $\gamma_a = \gamma_m = 0.05$ reaches relatively similar accuracy with KF-based algorithms for commonly dynamic tracking. However, when the motion is drastic, FCF will not be so accurate as KF.

The reason is that the complementary gain reamains fixed in our proposed FCF, and this is not appropriate for motion

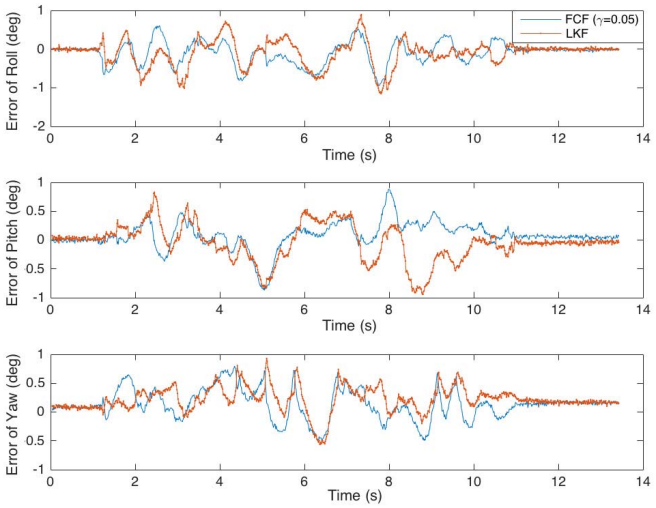

Fig. 7. Euler angles errors of the proposed FCF and LKF with respect to the golden reference. FCF with the two gains setting of 0.05 for this test case is comparable with LKF.

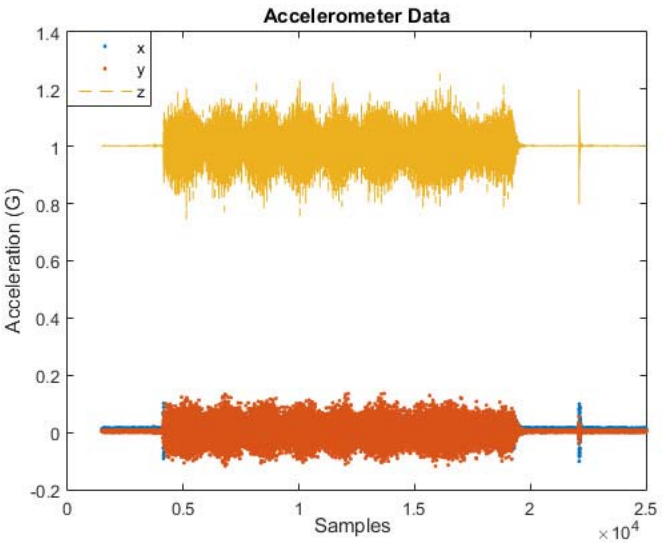

Fig. 8. The raw accelerometer data in the presence of vibration (80Hz).

modelling in highly dynamic conditions. However, Kalman filter consumes extensively greater computation time [16], making it unsuitable for cost-intensive applications. The avarage Mean Squared Errors (MSEs) of the three Euler angles from FCF and LKF with reference are 0.46770 and 0.43226 respectively. The result shows no significant difference between FCF and KF.

C. Vibration Test

AHRS has a high demand on the response in the presence of vibration. To demonstrate the performance of the proposed FCF under this condition, the designed experimental device is firmly attached to a vibration platform which mainly generates vibration in the vertical direction. In this case, the vibration frequency is set to 80Hz.

As shown in Fig. 8, the vibrational effect can be clearly observed from the accelerometer's output. Throughout Fast

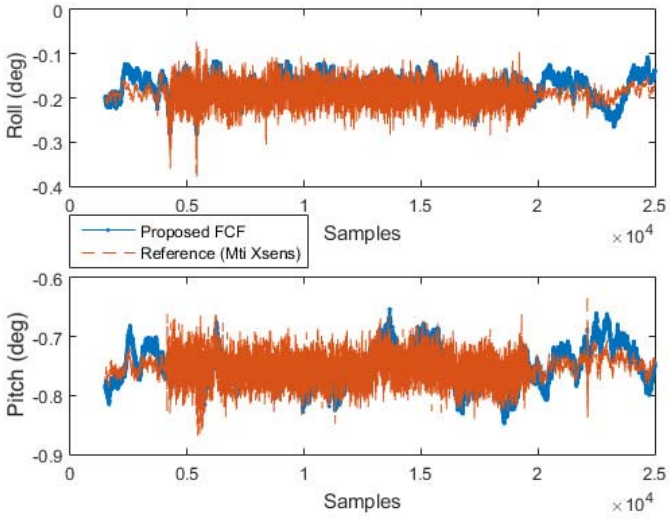

Fig. 9. The attitude angles from FCF and golden reference in the presence of vibration. The filter gain in this case is chosen as $\gamma_a = 0.01$.

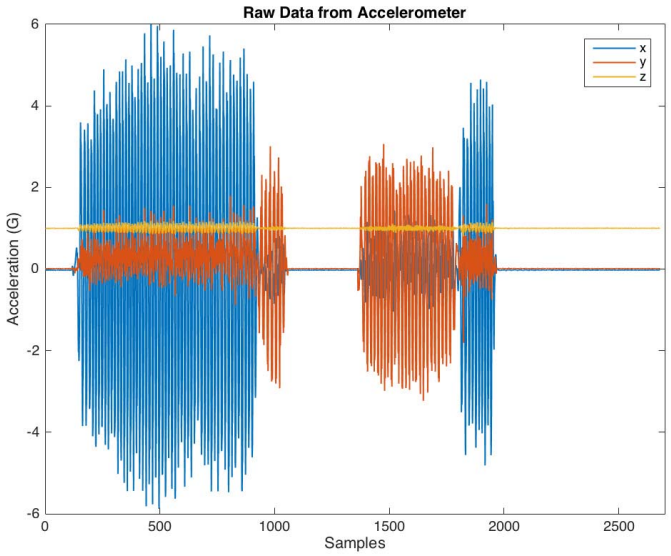

Fig. 10. The raw accelerometer's outputs consisting of large external acceleration.

Fourier Transformation (FFT) analysis, the vibration frequency of the a_z is about 75 to 82 which verifies the set value. Due to ferro-magnetic disturbance generated by the vibration platform, the magnetometer's data is not adopted in algorithm update. The fused attitude under this vibrational condition is depicted in Fig. 9.

Since the magnetometer is not adopted, only roll and pitch angles are estimated using the first CF. We can see that although the filter gain is fixed as 0.01, it owns relatively good anti-vibration ability compared with golden reference angles from MTi Xsens AHRS. This proves the robustness of the proposed FCF when vibration takes place. The overall statistical values of the two angles are shown in Table I.

D. Motion With Large External Acceleration

When large external acceleration takes place, the estimation error becomes more evident. In this case, the attitude determination from accelerometer would no longer be reliable.

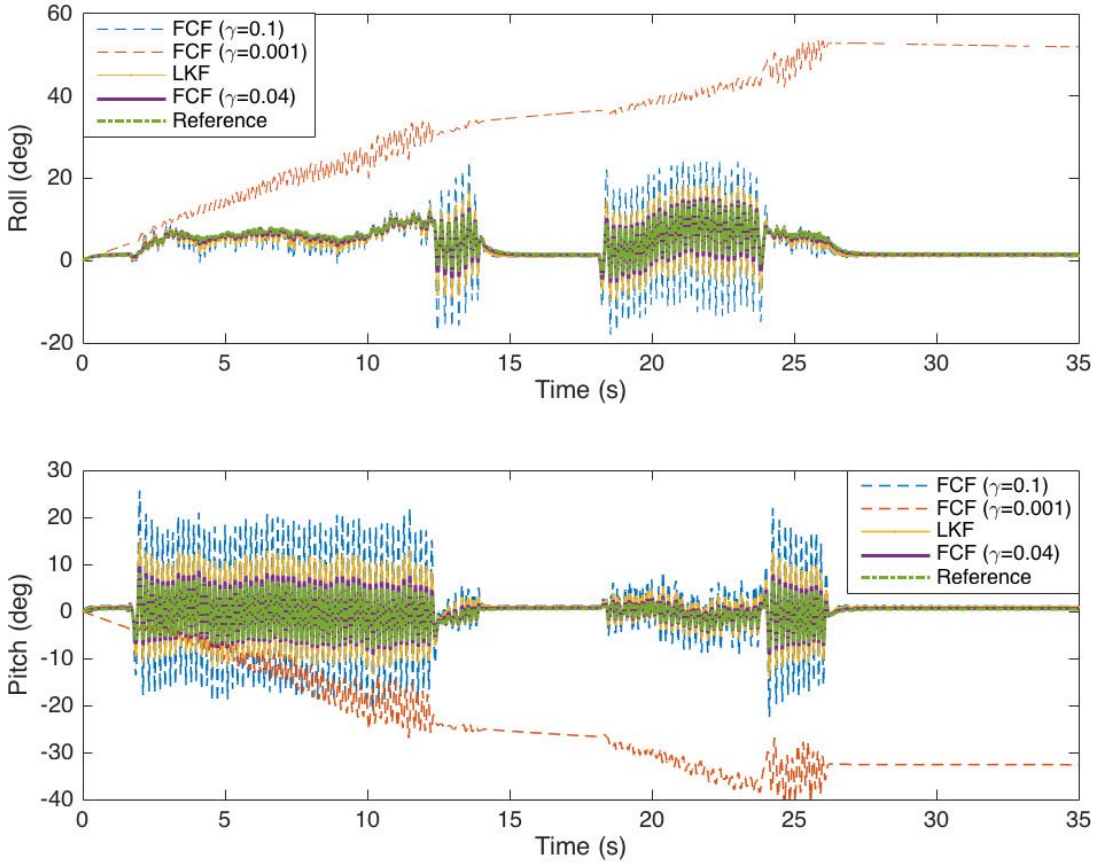

Fig. 11. Attitude estimation results from different sources in the presence of large external acceleration. Among all, the FCF with $\gamma_a = \gamma_m = 0.04$ owns the best estimation ability with respect to the reference angles.

TABLE I
VARIANCES AND MEAN VALUES OF ROLL AND PITCH ANGLES

Sources	Variance (Roll)	Variance (Pitch)
Reference	6.4844×10^{-4}	0.0010
Proposed FCF	5.1760×10^{-4}	5.7899×10^{-4}
Sources	Mean (Roll)	Mean (Pitch)
Reference	$-0.7533°$	$-0.1820°$
Proposed FCF	$-0.7542°$	$-0.1909°$

It is necessary to study the performances of various algorithms under such conditions. In this sub-section, the motion is generated using human hands on a table. The measured acceleration in this case is depicted in Fig. 10.

We can see that the scale of the acceleration is much bigger than that in the previous case. This in fact models another harsh environment for attitude estimation. Moreover, using the quaternion outputs from the golden reference, the estimated external acceleration can be calculated (see Fig. 12). This figure shows that the external acceleration is the main part of the accelerometer signal in this case. In this way, the mainly affected angles are roll and pitch.

The LKF and proposed FCF are used for validation. To give clear comparisons, FCFs with different gains are adopted. The estimated roll and pitch angles are shown in Fig. 11. As depicted in this figure, the gains of the proposed FCF significantly influence the attitude estimation performance.

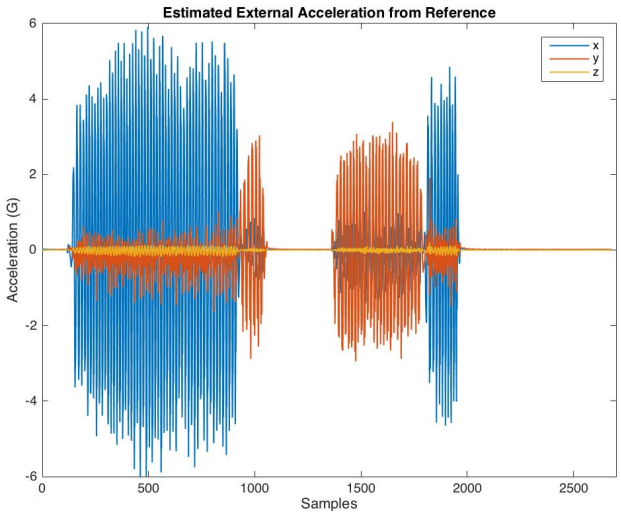

Fig. 12. The estimated external acceleration from reference angles. The external acceleration is mainly on the x and y axes.

When $\gamma_a = \gamma_m = 0.1$, the estimated attitude angles are drastic. This is because in this circumstance the accelerometer has a relatively big weight thus the filter is easily disturbed by external acceleration. However, when the gains are changed to $\gamma_a = \gamma_m = 0.04$, we may see that the estimated Euler angles are basically the same with reference angles. Besides, then the gains are very tiny ($\gamma_a = \gamma_m = 0.001$), the accelerometer can hardly compensate for the gyroscope's drift. This leads to the

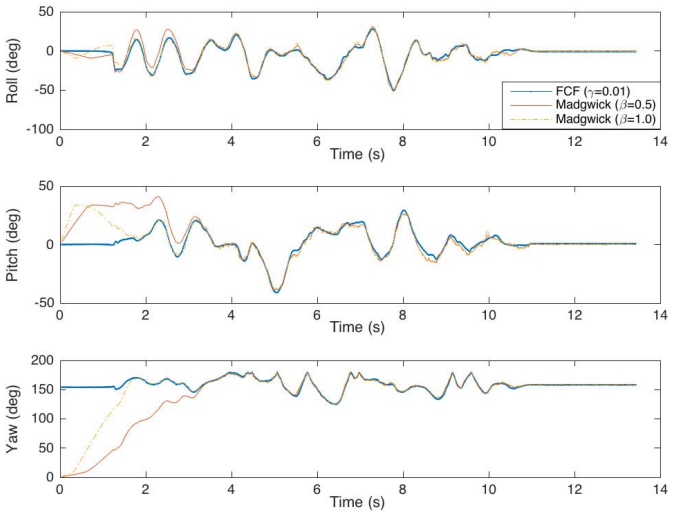

Fig. 13. Comparison with Madgwick's complementary filter with gains of $\beta = 0.5$ and $\beta = 1$.

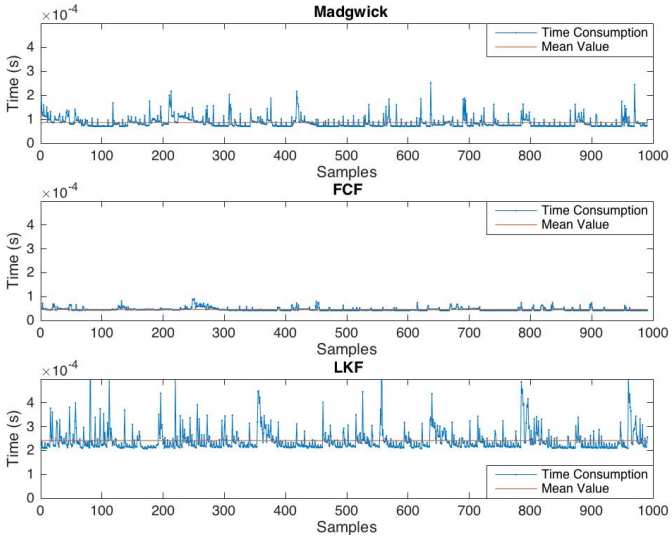

Fig. 14. Time consumption of Madgwick's complementary filter, the proposed FCF and Valenti's LKF. The average time consumption of the FCF is the least.

associated result in Fig. 11. From the red lines we can find out that the filter can no longer converge properly. All these results show that the proposed FCF is comparable with KF subject to some certain gains. However, in real applications the gains can be fixed when the filter is initialized. The research on the adaptive gains should be another task for us in the future.

E. Convergence Speed

In this section, we would like to verify the convergence performance of the proposed filter along with other iterative approach. A frequently used CF is the GDA-based filter by Madgwick et al. For the proposed FCF and Madgwick's filter, $\mathbf{q}_{t=0} = (1, 0, 0, 0)^T$ is set as the initial quaternion. The updates are conducted at the same time under MATLAB. Fig. 13 shows a slow convergence speed of the iterative CF.

Madgwick's algorithm uses a single iteration during each update in order to save computing time. This strategy remains valid only when the motion is not dynamic. Therefore the iterative method produces larger error than the proposed FCF method in the initializing regions. In contrast, the proposed FCF algorithm is free of iteration, thus the convergence problem caused by initial misalignment does not exist.

Also iterative based CFs are sensitive to filter gain. As depicted in Fig. 13, filter gain of $\beta = 0.5$ consumes nearly twice as much time to converge to the final value as $\beta = 1.0$. Larger gain may cause the filter to act quickly as the object moves but it would lower the effect of the gyroscope imposing on the estimator, which makes the estimator unreliable when large external acceleration takes place.

F. Comparison on Time Consumption

Time consumption is another critical indicator of the algorithm besides accuracy. Here we plot the time consumed by three algorithms in Fig. 14. By comparing the average time consumption, we notice that LKF consumes the most, approximately over twice as much as the other two, while FCF costs less than Madgwick's. This is because the LKF needs mass matrix operations e.g. multiplication and inversion while

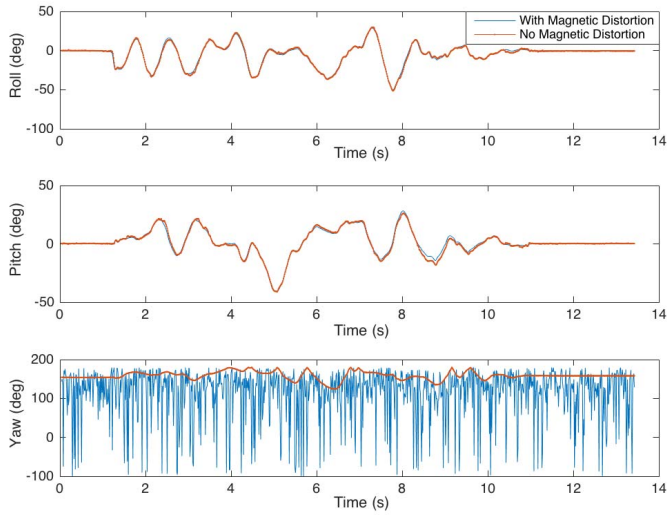

Fig. 15. Simulated attitude angles with gravity and distorted magnetic field. The roll and pitch angles are not influenced in this occasion.

Madgwick's filter requires computation of the Jacobian matrix, which are both absent in our proposed FCF. The FCF reaches a balance between the time consumption and accuracy. Hence, improvement in the time consumption enables the FCF more suitable than LKF and iterative CFs in some low-configuration embedded applications where computing resources and power are very limited.

G. Magnetic Distortion Simulation

When operating under magnetically distorted environment, the magnetometer's output will be heavily disturbed. A simulation is carried out using a distorted magnetic field and gravity to form the attitude quaternion with (43). However, as shown in Fig. 15, that magnetic distortion only affects yaw angle, while roll and pitch angles are free of impact. This is because roll and pitch angles are derived from the accelerometer and gyroscope, while magnetometer is only used to correct the heading.

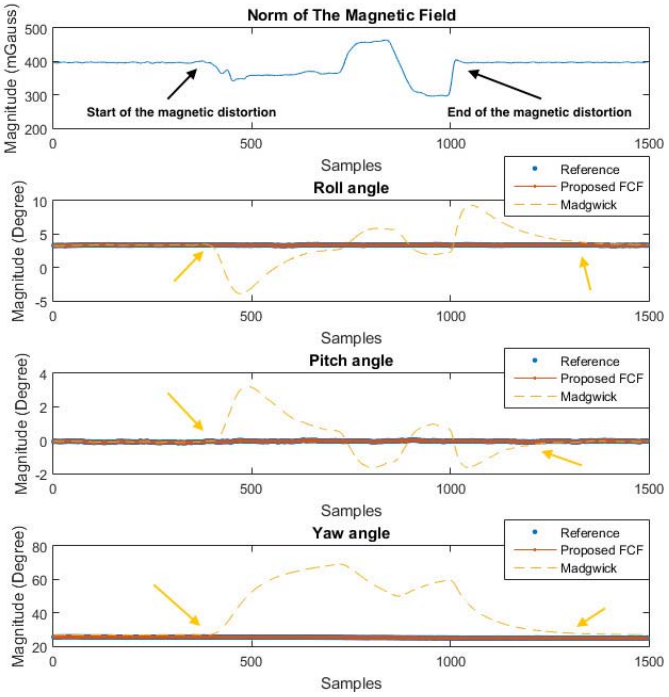

Fig. 16. Estimated attitude angles when unknown magnetic distortion takes place. The black arrows indicate the start and end of magnetic distortion while the yellow ones stand for the period of the Madgwick's reponse. The gains of the FCF are $\gamma_a = \gamma_m = 0.01$. Madgwick's filter's gain is chosen as $\beta = 0.5$.

Apart from this, another experiment is conducted on the designed experimental platform, where the magnetic field is distorted with an iron object. The norm of the measured magnetic field is shown in Fig. 16.

It can be seen that due to the algorithm's design, the proposed FCF can detect the magnetic distortion intelligently with the norms of the magnetometer's outputs. Thus it makes the yaw angles immune to external disturbances. However, the Madgwick's filter can be easily impacted, not only for the yaw angle but also for the other two angles. This result reassures robustness of our algorithm in challenged conditions with serious unknown magnetic distortion.

VI. Conclusion

The accelerometer-based attitude determination is derived as a linear system. Using knowledge of control systems, the solution to the linear system is successfully obtained. The proposed solution is fast and it is free of iterations. With this solution, a fixed-gain fast CF (FCF) which fuses gyroscope and accelerometer together is investigated and discussed. A second CF is further designed to fuse the magnetic outputs when magnetic distortion is not detected. By carrying out several experiments, the effectiveness of the proposed FCF on time consumption, accuracy, convergence speed and robustness when vibration and magnetic distortion take place is verified. The results show that FCF maintains a balance between the accuracy and time consumption. Although it is not so accurate as KF, it should be noted that the advantage in calculation-complexity is well worth the compromising accuracy of the attitude algorithm. The attitude errors of the proposed FCF are just slightly larger than that of the KF. As the complementary gain is fixed, the real-time motion-tracking ability is not so good as KF-based methods under highly dynamic conditions. The research on the adaptive-gain CF would be the future task.

Acknowledgment

Yunkan Technology Inc., Chengdu, China, provided test and calibration service for us. Prof. Yuhua Cheng and Prof. Bin Gao gives many important suggestions on revision. Liming Zhu verified the equations in this paper. We genuinely thank them for their support.

References

[1] Y. Cheng, L. Tian, C. Yin, X. Huang, and L. Bai, "A magnetic domain spots filtering method with self-adapting threshold value selecting for crack detection based on the MOI," *Nonlinear Dyn.*, 2016. [Online]. Available: http://link.springer.com/10.1007/s11071-016-2918-7

[2] W. Li and J. Wang, "Effective adaptive Kalman filter for MEMS-IMU/magnetometers integrated attitude and heading reference systems," *J. Navigat.*, vol. 66, no. 1, pp. 99–113, 2012.

[3] A. M. Sabatini, "Quaternion-based extended Kalman filter for determining orientation by inertial and magnetic sensing," *IEEE Trans. Biomed. Eng.*, vol. 53, no. 7, pp. 1346–1356, Jul. 2006.

[4] H. Fourati, "Heterogeneous data fusion algorithm for pedestrian navigation via foot-mounted inertial measurement unit and complementary filter," *IEEE Trans. Instrum. Meas.*, vol. 64, no. 1, pp. 221–229, Jan. 2015.

[5] N. Barbour and G. Schmidt, "Inertial sensor technology trends," *IEEE Sensors J.*, vol. 1, no. 4, pp. 332–339, Dec. 2001.

[6] J. Leclerc, "MEMS for aerospace navigation," *IEEE Aerosp. Electron. Syst. Mag.*, vol. 22, no. 10, pp. 31–36, 2007.

[7] Z. Zhou, Y. Li, J. Zhang, and C. Rizos, "Integrated navigation system for a low-cost quadrotor aerial vehicle in the presence of rotor influences," *J. Surv. Eng.*, vol. 4, pp. 1–13, May 2016.

[8] Z. Zhou, Y. Li, J. Liu, and G. Li, "Equality constrained robust measurement fusion for adaptive kalman-filter-based heterogeneous multi-sensor navigation," *IEEE Trans. Aerosp. Electron. Syst.*, vol. 49, no. 4, pp. 2146–2157, Oct. 2013.

[9] A. Makni, H. Fourati, and A. Y. Kibangou, "Energy-aware adaptive attitude estimation under external acceleration for pedestrian navigation," *IEEE/ASME Trans. Mechatronics*, vol. 21, no. 3, pp. 1366–1375, Jun. 2016.

[10] B. Li, Y. Shen, and L. Lou, "Efficient estimation of variance and covariance components: A case study for GPS stochastic model evaluation," *IEEE Trans. Geosci. Remote Sens.*, vol. 49, no. 1, pp. 203–210, Jun. 2011.

[11] J. Calusdian, X. Yun, and E. Bachmann, "Adaptive-gain complementary filter of inertial and magnetic data for orientation estimation," in *Proc. IEEE Int. Conf. Robot. Autom.*, May 2011, pp. 1916–1922.

[12] J. Cockcroft, J. H. Muller, and C. Scheffer, "A complementary filter for tracking bicycle crank angles using inertial sensors, kinematic constraints, and vertical acceleration updates," *IEEE Sensors J.*, vol. 15, no. 8, pp. 4218–4225, Aug. 2015.

[13] H. Fourati, N. Manamanni, L. Afilal, and Y. Handrich, "Complementary observer for body segments motion capturing by inertial and magnetic sensors," *IEEE/ASME Trans. Mechatronics*, vol. 19, no. 1, pp. 149–157, Feb. 2014.

[14] S. O. H. Madgwick, A. J. L. Harrison, and R. Vaidyanathan, "Estimation of IMU and MARG orientation using a gradient descent algorithm," in *Proc. IEEE Int. Conf. Rehabil. Robot.*, Jun./Jul. 2011, pp. 1–7.

[15] R. Mahony, T. Hamel, and J.-M. Pflimlin, "Nonlinear complementary filters on the special orthogonal group," *IEEE Trans. Autom. Control*, vol. 53, no. 5, pp. 1203–1218, Jun. 2008.

[16] Y. Tian, H. Wei, and J. Tan, "An adaptive-gain complementary filter for real-time human motion tracking with MARG sensors in free-living environments," *IEEE Trans. Neural Syst. Rehabil. Eng.*, vol. 21, no. 2, pp. 254–264, Mar. 2013.

[17] J. F. Vasconcelos, B. Cardeira, C. Silvestre, P. Oliveira, and P. Batista, "Discrete-time complementary filters for attitude and position estimation: Design, Analysis and experimental validation," *IEEE Trans. Control Syst. Technol.*, vol. 19, no. 1, pp. 181–198, Jan. 2011.

[18] R. Kannan, "Orientation estimation based on LKF using differential state equation," *IEEE Sensors J.*, vol. 15, no. 11, pp. 6156–6163, Nov. 2015.
[19] G. Ligorio and A. M. Sabatini, "A novel Kalman filter for human motion tracking with an inertial-based dynamic inclinometer," *IEEE Trans. Biomed. Eng.*, vol. 62, no. 8, pp. 2033–2043, Aug. 2015.
[20] A. M. Sabatini, "Kalman-filter-based orientation determination using inertial/magnetic sensors: Observability analysis and performance evaluation," *Sensors*, vol. 11, no. 10, pp. 9182–9206, 2011.
[21] R. G. Valenti, I. Dryanovski, and J. Xiao, "A linear Kalman filter for MARG orientation estimation using the algebraic quaternion algorithm," *IEEE Trans. Instrum. Meas.*, vol. 65, no. 2, pp. 467–481, Feb. 2016.
[22] W. T. Higgins, "A comparison of complementary and Kalman filtering," *IEEE Trans. Aerosp. Electron. Syst.*, vol. 11, no. 3, pp. 321–325, May 1975.
[23] D. Gebre-Egziabher, R. C. Hayward, and J. D. Powell, "A low-cost GPS/inertial attitude heading reference system (AHRS) for general aviation applications," in *Proc. IEEE Position Location Navigat. Symp.*, Apr. 1998, pp. 518–525.
[24] J. A. Farrell, *Aided Navigation: GPS With High Rate Sensors*. New York, NY, USA: McGraw-Hill, 2008.
[25] M. J. Caruso, "Applications of magnetic sensors for low cost compass systems," in *Proc. IEEE Position Location Navigat. Symp.*, Mar. 2000, pp. 177–184.
[26] F. Liu, J. Li, H. Wang, and C. Liu, "An improved quaternion Gauss–Newton algorithm for attitude determination using magnetometer and accelerometer," *Chin. J. Aeronautics*, vol. 27, no. 4, pp. 986–993, 2014.
[27] H. Fourati, N. Manamanni, L. Afilal, and Y. Handrich, "A nonlinear filtering approach for the attitude and dynamic body acceleration estimation based on inertial and magnetic sensors: Bio-logging application," *IEEE Sensors J.*, vol. 11, no. 1, pp. 233–244, Jan. 2011.
[28] G. Wahba, "A least squares estimate of satellite attitude," *SIAM Rev.*, vol. 7, no. 3, p. 409, 1965.
[29] F. L. Markley, "Fast quaternion attitude estimation from two vector measurements," *J. Guid., Control, Dyn.*, vol. 25, no. 2, pp. 411–414, 2002.
[30] F. L. Markley and J. L. Crassidis, *Fundamentals of Spacecraft Attitude Determination and Control*. New York, NY, USA: Springer, 2014.
[31] X. Yun, E. R. Bachmann, and R. B. Mcghee, "A simplified quaternion-based algorithm for orientation estimation from earth gravity and magnetic field measurements," *IEEE Trans. Instrum. Meas.*, vol. 57, no. 3, pp. 638–650, Mar. 2008.
[32] F. L. Markley and D. Mortari, "How to estimate attitude from vector observations," *Adv. Astron. Sci.*, vol. 103, no. 3, pp. 1979–1996, 2000.
[33] A. Jennings and J. J. McKeown, *Matrix Computation*. NEw York, NY, USA: Wiley, 1992.
[34] Analogs Device Inc. *ADIS16405 Datasheet*. [Online]. Available: http://www.analog.com/media/en/technical-documentation/data-sheets/ADIS16405.pdf

Jin Wu received the B.S. degree from University of Electronic Science and Technology of China, Chengdu, China, in 2016. He is currently a Research Assistant with the School of Aeronautics and Astronautics, School of Automation, University of Electronic Science and Technology of China. His research interests include inertial navigation, machine vision, control theory and applications.

Zebo Zhou received the B.Sc. and M.Sc. degrees in surveying and engineering from Wuhan University, in 2004 and 2006, respectively, and the Ph.D. degree from the College of Surveying and Geo-Informatics, Tongji University, Shanghai, China, in 2009. He is currently an Associate Professor with the School of Aeronautics and Astronautics, University of Electronic Science and Technology of China. His research interests include GNSS navigation and positioning, GNSS/INS integration, multi-sensor fusion, and surveying data processing theory.

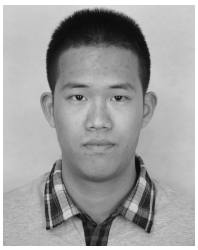

Jingjun Chen received the B.S. degree in electrical engineering from the Harbin Institute of Technology, Harbin, China, in 2016. He is currently pursuing the M.S. degree with the University of California at Davis, Davis.

His research interests include electrical engineering, sensor fusion, and automated electronics.

Hassen Fourati received the B.E. degree in electrical engineering from the National Engineering School of Sfax, Tunisia, in 2006, the master's degree in automated systems and control from University Claude Bernard, Lyon, France, in 2007, and the Ph.D. degree in automatic control from the University of Strasbourg, France, in 2010. He is currently an Associate Professor of Electrical Engineering and Computer Science with University Grenoble Alpes, Grenoble, France. His research interests include nonlinear filtering and estimation and multisensory fusion with applications in navigation, robotics, and traffic management. He is a member of the Networked Controlled Systems Team, affiliated with the Automatic Control Department, GIPSA-Laboratory.

Rui Li (M'10) received the Ph.D. degree in control science and engineering from the Harbin Institute of Technology, China, in 2008. She was with the University of Electronic Science and Technology of China in 2008, where she is currently an Associate Professor in School of Automation. She was a Visiting Research Associate with the Department of Applied Mathematics, The Hong Kong Polytechnic University, and the Department of Mathematics and Statistics, Curtin University of Technology. From 2011 to 2012, she was a Visiting Scholar with the Department of Electrical Engineering, University of California at Riverside. Her research interests include optimization theory and optimal control, nonlinear control, multi-agent systems, and aircraft control.